

Thermal conductivity of the cell membrane in the presence of cholesterol and amyloid precursor protein

Neda Rafieiolhosseini *

School of Nano Science, Institute for Research in Fundamental Sciences (IPM), P. O. Box 19395-5531, Tehran, Iran

Mohammad Reza Ejtehadi †

Department of Physics, Sharif University of Technology, Tehran 11365-11155, Iran

 (Received 4 April 2020; revised 13 August 2020; accepted 16 September 2020; published 5 October 2020; corrected 10 November 2020 and 30 March 2021)

The cell membrane is responsible for the transportation of heat between inside and outside the cell. Whether the thermal properties of the cell membrane are affected by the cholesterol concentration or the membrane proteins has not been investigated so far. Although the experimental measurement of the membrane thermal conductivity was not available until very recently, computational methods have been widely used for this purpose. In this study, we carry out molecular dynamics simulations to investigate the relation between the concentration of cholesterol and the thermal conductivity of a model membrane. Our results suggest an increase in the membrane thermal conductivity upon increasing the concentration of cholesterol in the membrane. Moreover, we find that the asymmetric distribution of cholesterol in the two membrane leaflets decreases thermal conductivity. We also find a rectification effect when heat flows in opposite directions through a model membrane decorated with the amyloid precursor protein. The results of this study apply to the advancement of selective treatment methods, as well as the development of new materials such as biological rectifiers.

DOI: [10.1103/PhysRevE.102.042401](https://doi.org/10.1103/PhysRevE.102.042401)

I. INTRODUCTION

The cell membrane, as the outermost part of a cell, plays an important role in controlling the exchange of material and heat between inner and outer parts of a cell. Although all membranes roughly consist of lipid molecules (including phospholipids and cholesterol), proteins, and carbohydrates [1], the concentration of each constituent is different in different types of cells. It is evident that the properties of the membrane depend highly on the membrane composition [2]. For instance, the structural properties of the membrane, such as its rigidity, depend on the concentration of cholesterol which is normally between 10 and 45 molar percentage of total lipids in the membrane [3]. In some types of cells, however, the distribution of cholesterol is different in the inner and outer leaflets of the membrane. In red cells, for example, the percentage of cholesterol in the outer leaflet is 51% and in the inner leaflet is 49% [4]. In other types of cells, such as colorectal cells, cholesterol constitutes about 2.77% of the inner leaflet and 33.3% of the outer leaflet in healthy cells. In other words, in the membrane of healthy colorectal cells, the ratio of $[CHL]_o$ to $[CHL]_i$ usually is 12, while it decreases to 5.5 in the membrane of cancerous colorectal cells [3]. Proteins are the other important building blocks of the cell membrane and do a variety of tasks. They are divided into two main categories: integral membrane proteins (embedded

in the membrane) and peripheral membrane proteins (located on the membrane surface) [5–7]. Integral membrane proteins interact with membrane via their transmembrane domain, which mostly consists of hydrophobic amino acids. Amyloid precursor protein (APP) is a well-known example of integral membrane proteins [8,9]. More than half of the mutations in APP associated with Alzheimer’s disease occur in the transmembrane domain of this protein [10].

Thermal conductivity is one of the important physical properties of the cell membrane. Thermal conductivity measurements of the membrane can be useful for engineering new materials, such as nanoparticles, to be used in modern treatment techniques. For instance, in a selective treatment method called photothermal cancer therapy, metal nanoparticles inside the tissue generate heat after being radiated by an external source. The generated heat then transports to the nearby cells through the cell membrane [11]. To tune the parameters (such as the power) of the radiative source properly and to achieve high efficiency, one should have an understanding of the thermal conductance and resistance of the cell membranes.

The thermal conductivity of the cell membrane has been measured in a very recent experiment [12] using an approach called luminescence thermometry. In this method, upconverting nanoparticles covered by lipid bilayers are used as heat sources while the environmental fluid acts as a heat sink. A thermocouple, which is immersed in the fluid, measures the temperature of the environment. The difference between the temperatures of nanoparticles and fluid is used to calculate the thermal conductivity of the intermediate lipid bilayer.

Although the experimental measurement of the membrane thermal conductivity has not been reported until very recently, several computational techniques have been developed and

*ne.rafiiee@gmail.com; present address: Bioinformatics and Computational Biophysics, Faculty of Biology, University of Duisburg-Essen, Essen, Germany.

†ejtehadi@sharif.edu

utilized to compute the thermal conductivity of lipid bilayers so far. The nonequilibrium molecular dynamics (NEMD) algorithm developed by Müller-Plathe [13] has been employed to obtain the local thermal conductivity coefficient of heterogeneous dipalmitoylphosphatidylcholine (DPPC) lipid bilayer [14]. The results suggest that the value of thermal conductivity is a minimum in the region between two membrane leaflets where the alkyl chains meet. A possible reason for such a high thermal resistance could be the lack of a covalent bond in the area between the two membrane leaflets [15]. An asymmetry in thermal conductivity is also reported in the same paper. Other studies supported the idea of asymmetric heat conductance through lipid membranes as well as a discontinuity in the thermal conductivity profile where lipid tails touch [16,17]. Furthermore, different thermal conductivity coefficients in normal and lateral directions of a bilayer have been reported [16]. A nonequilibrium molecular dynamics approach has been used to study the thermal conductivity and rectification of asymmetric archaean membranes as well [18]. Three types of archaeols with the same head group but different tail structures (with and without cyclopentane rings) have been investigated, and the area per lipid molecule has been considered as a measure of the compactness of lipid molecules. According to the results of the same study, cyclopentane rings are responsible for the high level of molecular packing and the increase in the thermal conductivity of the membrane.

Several studies report the condensation effect, which is a structural change in the membrane upon the addition of cholesterol molecules [19,20]. Condensation means that the area per lipid molecule decreases to less than the weighted average of areas of pure components [20]. The reason is that cholesterol interacts with lipids via hydrogen bonding and can fill the voids between lipid molecules [21]. The higher the percentage of cholesterol, the smaller the area per lipid molecule. Furthermore, cholesterol affects the phase behavior of phospholipid membranes in a concentration-dependent manner [22]. In cholesterol concentrations less than 25%, the membrane is always in one of the liquid-disordered or solid-ordered phases, depending on the temperature. However, in higher levels of cholesterol, the membrane can be found only in one phase called the liquid-ordered phase. It is also evident that the effect of cholesterol on the structural order of the membrane depends on the temperature. Above the phase transition temperature at which lipids are in the liquid phase, the addition of cholesterol to the membrane increases the structural order, while below this temperature lipids are in the gel phase and the addition of cholesterol disrupts the order [22].

This study takes a computational approach to investigate the thermal conductivity of the cell membranes with different compositions: at different levels of cholesterol and in the presence of APP. The motivation behind this is, on the one hand, the dependence of thermal conductivity on the structure, and on the other hand, the relation between the level of cholesterol in the membrane and the membrane structure [20,22].

To have an understanding of thermal transport in membranes with the ratio $[CHL]_o/[CHL]_i \neq 1$, we extend our study to a model membrane with a ratio of $[CHL]_o/[CHL]_i = 12$, such as the one for normal colorectal cells. The idea behind this comes from a recent investigation

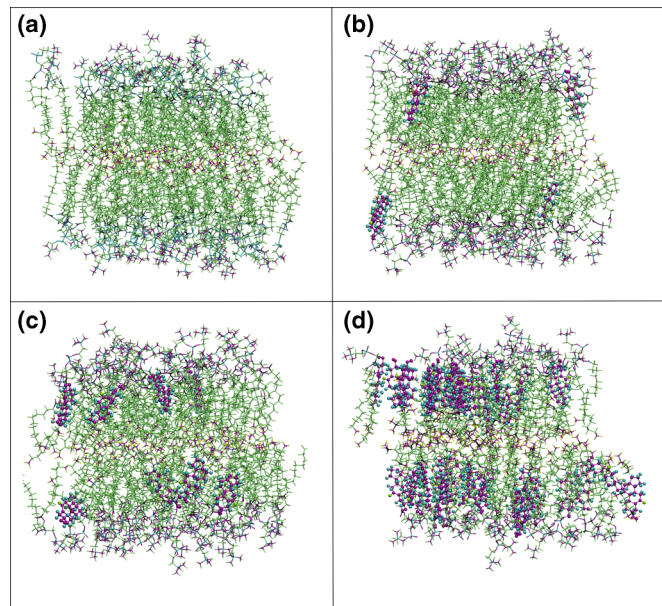


FIG. 1. Pre-equilibrated DPPC lipid membranes with different cholesterol concentrations: (a) 0% cholesterol, (b) 5% cholesterol, (c) 11% cholesterol, and (d) 50% cholesterol. Each membrane leaflet consists of 36 lipids including DPPC and cholesterol molecules. DPPC molecules are represented with lines in green and cholesterol molecules are represented with ball-and-stick in blue and purple.

on thermal conductivity and rectification of asymmetric archaean membranes [18].

Results of a previous study suggest that a slight change in temperature affects the interaction of the amyloid protein with hydrophobic and hydrophilic surfaces [23]. Considering the sensitivity of this protein to the temperature, many questions arise about the reaction of this protein to a temperature gradient and how the local temperature profile (and therefore thermal conductivity) can be affected by this protein. Here we study a model DPPC membrane containing the trans-membrane part of APP. We also consider another DPPC membrane with a horizontally laid APP on its surface. For these models, we obtain the rectification factor, which is a measure of the difference between the thermal conductivity coefficients when heat flows in the opposite directions through the membrane.

This paper is divided into the following sections. In Sec. II we describe the method that we used to obtain the thermal conductivity coefficient of membranes and discuss the technical details of our simulations. In Sec. III we report and discuss our results. Finally, we conclude and summarize the main points in Sec. IV.

II. METHODS

To investigate the effect of cholesterol on the thermal conductivity of the membrane, an atomistic model of DPPC lipid bilayer is used (Fig. 1). Each of the inner and outer leaflets contains 36 lipid molecules some of which are cholesterol molecules corresponding to the given concentrations (0%, 5%, 11%, and 50%). It should be mentioned that the concentration of cholesterol in the inner and outer membrane

leaflets is the same in all of these models. Although the thermal conductivity coefficient of the DPPC membrane without cholesterol is reported in the previous computational studies [14,24], we repeat it here not only to validate our model but also to have a reference value for the evaluation of the thermal conductivity of the membranes containing cholesterol.

As the initial step for all the simulations, the pre-equilibrated structures of lipid bilayers are obtained from the CHARMM-GUI membrane builder [25]. Output files produced by the CHARMM-GUI apply to a variety of molecular dynamics simulation packages. Here we use the LAMMPS molecular dynamics package [26] for all simulations. Interactions between lipid-lipid, lipid-protein, and lipid-water molecules are treated using the CHARMM36 force field [27,28], and the TIP3P [29] model is used to model water. To find the thermal conductivity and rectification of the membranes decorated with the amyloid precursor protein, initial structures of the transmembrane part of the APP (PDB code 2llm [10]) and part of the APP that lies on the membrane surface (PDB code 2lp1[30]) are obtained from protein databank [31,32] and used as the input to the OPM database [33], which provides the orientation of proteins in the membrane. The oriented structure of the protein is fed into the CHARMM-GUI membrane builder to be packed with the specific types of lipid molecules. Finally, the Moltemplate plug in is used to locate the membrane in the right place in the simulation box and to fill the box with the appropriate number of ions and water molecules [34].

In this study, all the simulations are done in two parts. In the first part, an equilibrium molecular dynamics simulation is performed, while in the second part, a nonequilibrium molecular dynamics approach is used to compute the thermal conductivity coefficient.

A. Equilibrium molecular dynamics

Each system undergoes an energy minimization and equilibration process. To reduce the large forces due to the possible overlaps between atoms, we run the energy minimization for 10 000 steps for each system. The conjugate gradient method is used to minimize the initial structures. Moreover, to relax the structures, all of the membranes undergo the equilibration process at a high temperature (450 K) and pressure (170 bar) using Langevin dynamics. The equilibration procedure starts with a very small time step (0.01 fs) and is done only for a few steps (1000 steps). We increase time step and the number of steps gradually to reach the time step of 1 fs. (The equilibration is done for 1000 steps at 0.01 fs, followed by 1000 steps at 0.05 fs, followed by 1000 steps at 0.1 fs, followed by 2000 steps at 0.2 fs, followed by 5000 steps at 0.5 fs, followed by 100 000 steps at 1.0 fs.) The equilibration process is then continued by another 1 ns under NPT condition at temperature 330 K and pressure 1 bar to stabilize the area per lipid molecule. The values of the area per lipid are then evaluated with the previously reported values [19]. The systems are kept at $T = 330$ K, which is above the phase transition temperature of DPPC (314 K) [35], and the system pressure is adjusted to 1 bar using an isotropic Nose-Hoover barostat [36].

To build the appropriate simulation box for the implementation of the NEMD approach and to have a correct periodic

TABLE I. Dimensions of the simulation box and the number of atoms in each box for different model membranes used in this study.

System	Δx (Å)	Δy (Å)	Δz (Å)	Number of atoms
0% cholesterol	48.0	46.0	184.2	42 804
5% cholesterol	47.4	45.0	186.3	41 756
11% cholesterol	45.0	46.6	188.4	41 476
50% cholesterol	42.2	38.8	194.2	33 762
Asymmetric cholesterol	44.4	44.4	180.0	36 338
App on the membrane	54.4	54.2	187.0	57 734
App across the membrane	46.6	46.6	170.6	39 132

boundary condition along the z axis, the model membrane and its mirror image are located parallel to each other in the simulation box, which is filled with the appropriate number of water molecules. Finally, to relax the water molecules and to let the final simulation box find the correct volume and density, we equilibrate the systems once more (only for a short period on the order of some hundreds of picoseconds). The same equilibration procedure as the one applied to the single lipid bilayer is used to equilibrate the double lipid bilayer in the box. Table I shows dimensions and the number of atoms in the final simulation boxes for the model membranes used in this study.

B. Thermal conductivity calculation (nonequilibrium molecular dynamics)

There are two possible approaches to obtain the thermal conductivity of a material. In the first approach, which is called the direct method, one can create a temperature gradient across the system and measure the rate of heat flow throughout the system. The thermal conductivity coefficient is then obtained by dividing the rate of heat flow to the temperature gradient. Because of some drawbacks, including highly fluctuating heat flow and slow convergence of the system, an alternative method is to continuously apply a nonphysical heat flux to the system until a physical heat flux establishes throughout the system. After some time, the physical and non-physical heat flow rates are equalized and the system reaches a so-called steady state. In this situation, a stable temperature gradient establishes across the system. This method is called reverse nonequilibrium molecular dynamics (RNEMD) [13].

To implement reverse nonequilibrium molecular dynamics in our study, we use the Müller-Plathe technique [13]. In this method, the simulation box is divided into several layers (Fig. 2). At each time step (or as many time steps as the user wants), the velocity of the hottest particle in the first layer in the box is exchanged with the velocity of the coldest particle in the middle layer of the box. Therefore, the exchange rate is a known, user-defined parameter. Since the total momentum should be kept conserved, only the particles with the same mass are allowed to exchange velocity. After a while, the first and the middle layers of the box change into the coldest and hottest layers, respectively. Consequently, a physical heat flow is established from the hot region to the cold region in the box. After the system reaches a steady state, the temperature gradient can be measured and used to calculate the thermal conductivity coefficient using Fourier law.

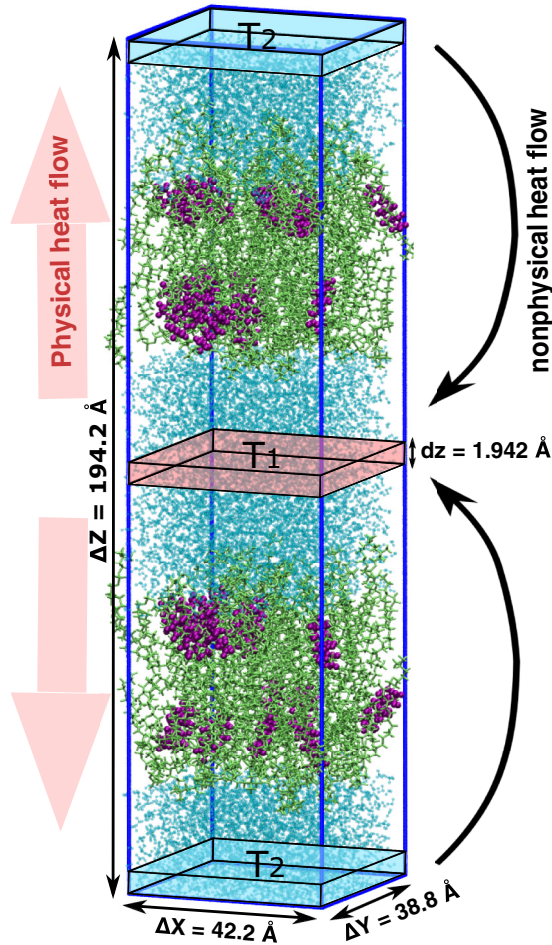


FIG. 2. Physical and nonphysical heat flow across the model membrane with 50% cholesterol concentration. The Müller-Plathe NEMD algorithm applies a nonphysical heat flow between two layers of the simulation box, specified with T_1 (hottest layer) and T_2 (coldest layer), which results in a physical heat flow across the lipid bilayers. Water layers with the highest and the lowest temperatures are colored in light red and light blue, respectively. In the two lipid bilayers, green lines and purple beads represent DPPC and cholesterol molecules, respectively.

1. Implementation of Müller-Plathe technique

We divide the simulation box into 100 layers. The thickness of one layer in the box varies between 1.8 Å to 1.9 Å in our simulations, depending on the height of the box. Further information about the box dimensions and the number of atoms in each system is given in Table I. Particles from the first and middle (51st) layers of the box are chosen for velocity exchange. By convention here, we consider that heat flows in the forward direction when the first layer of the box (indicated by T_2 in Fig. 2) has the lowest temperature, and the layer in the middle (indicated by T_1 in Fig. 2) has the highest temperature. Therefore, the heat flows from the center toward the two ends of the box. On the other hand, the backward direction is considered when heat flows from the two ends of the box toward the center. We exchange the velocities every 0.1 ps. With this exchange rate, we are always in the linear response regime. Accordingly, thermal conductivity coefficient

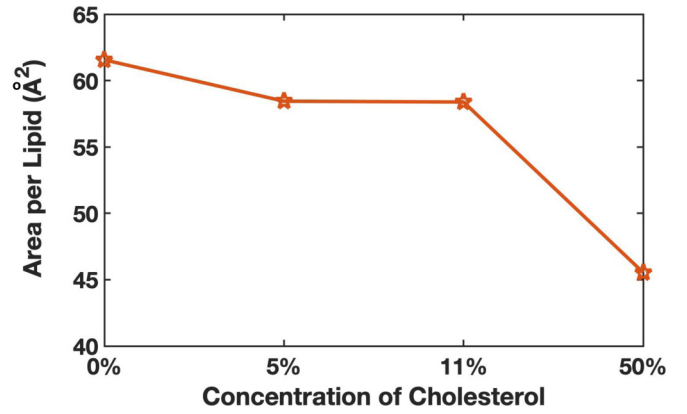


FIG. 3. Area per lipid molecule for DPPC membranes containing different concentrations of cholesterol. The numbers on the horizontal axis indicate the percentage of cholesterol in each leaflet of membranes.

is calculated using Eq. (1):

$$\kappa = -\frac{J}{\nabla T} = -\frac{1}{2} \frac{\frac{dQ}{Adt}}{\frac{dT}{dz}}, \quad (1)$$

where $\frac{dQ}{dt}$ is the rate of heat flow, dz is the distance between hot and cold layers in the box, dT is the difference between temperatures of hot and cold layers, and A is the cross-sectional area. Since heat flows in two opposite directions, one-half of the heat flow should be used for the calculation of the thermal conductivity coefficient (κ).

2. Estimation of thermal rectification factor

Thermal conductivity coefficients are obtained in forward and backward directions and used to calculate the thermal rectification factor using Eq. (2):

$$\varepsilon = \frac{|\kappa_f - \kappa_b|}{\kappa_b}, \quad (2)$$

where κ_f and κ_b are the thermal conductivity coefficients when heat flows in the forward and backward directions, respectively. We divide the total simulation time into the blocks with 1 ns length and calculate the thermal conductivity coefficient for each block. We applied the block averaging method to obtain the final values of the thermal conductivity coefficients.

III. RESULTS

A. Effects of cholesterol on the structure and thermal conductivity of the DPPC membrane

To investigate the effect of cholesterol on the structure of the DPPC membrane, the area per lipid molecule is obtained after the equilibration phase. An increase in the level of cholesterol in the membrane results in a reduction in the area per lipid molecule (Fig. 3 and Table I). It is reported in previous studies as well [20,37,38]. Furthermore, our findings suggest that the membranes with more cholesterol molecules have a higher thickness, which is in agreement with previous reports [39,40].

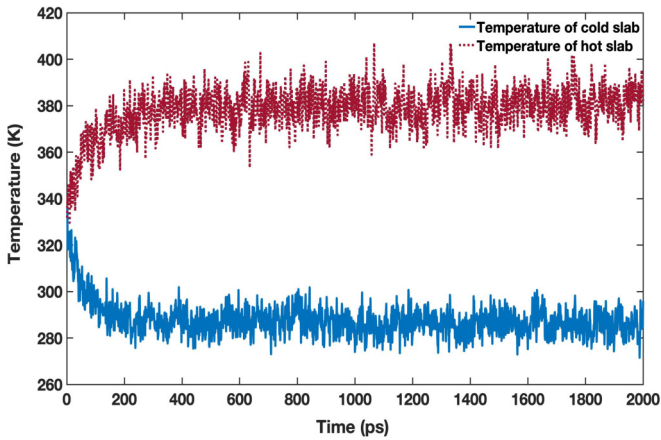


FIG. 4. Implementation of Müller-Plathe algorithm results in the formation of hot and cold regions in the box. This figure represents the first 2 ns of the NEMD simulation and implies that the temperature of the hot and cold slabs reaches a steady state in hundreds of picoseconds after NEMD starts with an exchange rate of 0.1 ps. All model membranes we use in this study have similar plots to this one.

Implementation of the Müller-Plathe algorithm leads to the creation of hot and cold slabs across the membrane. Temperatures of hot and cold slabs reach a steady state after some hundreds of picoseconds (Fig. 4). In our study, we do all the calculations on the data gathered after the first nanosecond of the simulations. Due to the exchange of velocities, a specific amount of kinetic energy is accumulated in each simulation step. If the velocities are exchanged slowly enough, the accumulated kinetic energy will be a linear (monotonically increasing) function of time. Otherwise, the system will never reach a steady state. The slope of this function gives the rate of heat flow. The density and temperature profiles of the system along the z axis (Fig. 5) suggest that in the hottest and coldest layers of the box there are only water molecules. It is worth mentioning that the two jumps in the temperature profile (Fig. 5), one in the region between slab number 20 and 30, and the other in between slab number 70 and 80, match exactly the two minimums in the membrane density profile

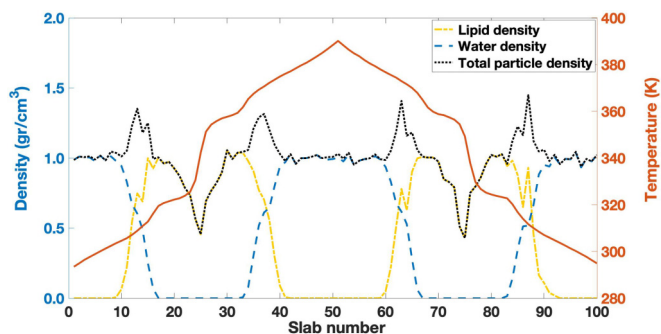


FIG. 5. Densities of water, lipid, and total particle density along the z axis are represented on the left vertical axis. The temperature of each layer when the system reaches the steady state is also represented on the right vertical axis. The overall density and temperature profiles of all model membranes we use in this study are similar to this one.

TABLE II. Result of the t test for membranes with different levels of cholesterol.

Systems	Mean diff.	Std. err. diff.	t	df	Sig. (2-tailed)
0%, 5%	-0.016	0.002	-7.692	38.0	$p < 0.001$
0%, 11%	-0.019	0.002	-10.958	42.0	$p < 0.001$
0%, 50%	-0.032	0.002	-17.346	43.0	$p < 0.001$
5%, 11%	-0.003	0.002	-1.161	36.0	$p = 0.241$
5%, 50%	-0.015	0.002	-6.546	37.0	$p < 0.001$
11%, 50%	-0.013	0.002	-6.589	41.0	$p < 0.001$

indicating the areas between the two membrane leaflets where lipid tails touch [14]. Density profiles in Fig. 5 indicate the density of particles before applying NEMD to the system. After NEMD is applied to the system, there is a slight change in the density of water with a lower density in the hot region and a higher density in the cold region. However, there is no change in the density of lipids.

We report the value of the thermal conductivity of the DPPC membrane to be $0.57 \pm 0.01 \text{ W m}^{-1} \text{ K}^{-1}$ at $\Delta T = 74 \text{ K}$, which is in good agreement with the computationally predicted value ($0.51 \pm 0.04 \text{ W m}^{-1} \text{ K}^{-1}$ at $\Delta T = 75 \text{ K}$) by Yousefian *et al.* [24]. To the best of our knowledge, the only experimentally measured value reported very recently is $0.20 \pm 0.02 \text{ W m}^{-1} \text{ K}^{-1}$ obtained for a membrane composed of DOPA:DOPC:cholesterol (with the ratio of 64:7:29) at $\Delta T = 20 \text{ K}$ [12]. The difference in the reported values of the membrane thermal conductivity is not only due to the different membrane compositions but also because of the difference in the applied temperature gradients across the membrane [12,24]. For instance, in a previous computational study, the thermal conductivity of $0.25 \text{ W m}^{-1} \text{ K}^{-1}$ was reported for a DPPC bilayer at $\Delta T = 12 \text{ K}$ [15].

According to the results of the t test (Table II), the presence of cholesterol in the membrane, especially in high concentration, increases the thermal conductivity of the lipid bilayer (see Fig. 6). The reason can be partly explained by the increased structural order in the membrane (in the liquid phase) due to the addition of cholesterol that is in total agreement with the previous reports [22]. These results suggest that the increase in the thermal conductivity of each two membranes (containing different levels of cholesterol) is statically significant (significance level = 0.05), except for the two membranes with cholesterol concentrations 5% and 11%.

B. Hydration of lipid head groups

Results of a previous experimental study [41] suggest that cholesterol affects membrane-water interaction by increasing the water penetration to the hydrophilic part of the membrane. Since the important role of the membrane-water interface in determining thermal conductivity of membrane has been emphasized in the literature, we investigate the hydration of lipid head groups in two of our model membranes: in the cholesterol-free membrane and in the membrane containing 50% cholesterol. We obtain the radial distribution function of water oxygen around the nitrogen atom of DPPC head groups (Fig. 7). According to the results, we conclude that

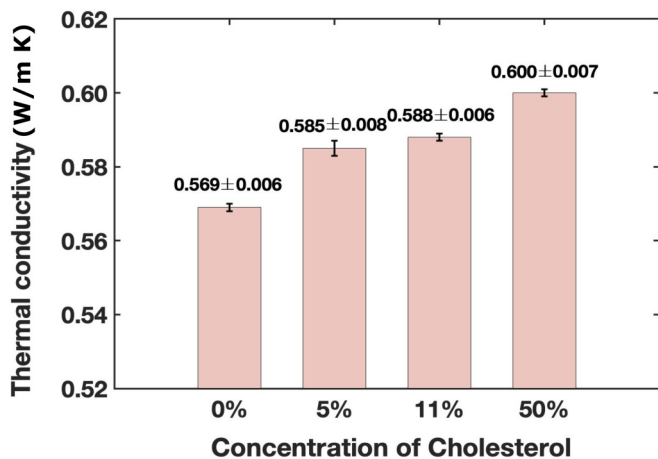


FIG. 6. Thermal conductivity coefficients of lipid membranes with different concentrations of cholesterol. Simulations are divided into several 1 ns time blocks, and the thermal conductivity coefficient is obtained in each block. The mean value (\pm standard deviation) written on top of each bar is obtained using the block averaging method. Error bars show the value of standard deviation divided by the square root of the number of blocks.

the hydration increased upon the inclusion of 50% cholesterol to the membrane.

C. Thermal conductivity and rectification of a DPPC membrane with different concentrations of cholesterol in the upper and lower leaflets

The asymmetric concentration of cholesterol in the membrane leaflets has been discussed in many studies [42,43]. To achieve more realistic results, this asymmetry should be taken into account in membrane models. In this study, we use a pre-equilibrated membrane with asymmetric cholesterol concentration in the two leaflets. Our model membrane contains 33.3% cholesterol in the outer leaflet and 2.7% cholesterol

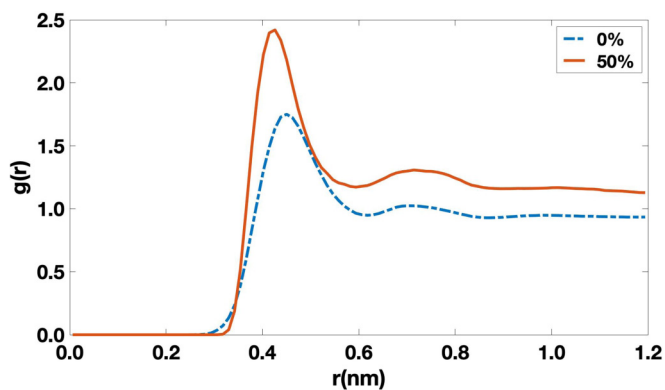


FIG. 7. Radial distribution function (RDF) of water oxygens around the nitrogen atom of DPPC head groups for two membranes: the cholesterol-free membrane (dashed blue curve) and the membrane containing 50% cholesterol (solid red line). A comparison between the peak values of the two RDFs reveals that the lipid head groups get more hydrated as a result of the incorporation of cholesterol into the membrane.

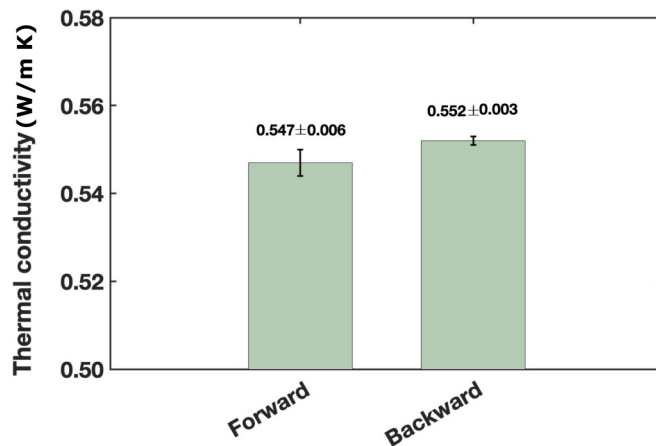


FIG. 8. Thermal conductivity coefficients for a DPPC membrane whose upper and lower leaflets contain different numbers of cholesterol molecules. Thermal conductivity values are obtained for this model in the forward and backward directions.

in the inner leaflet. We study the thermal conductivity of this model membrane in a forward and backward direction (Fig. 8).

The thermal conductivity coefficients obtained in both directions for this asymmetric model membrane are less than the values obtained for our aforementioned symmetric models. The asymmetry in the structure of the membrane leaflets might be the reason for the reduction in the thermal conductivity of the membrane. As a similar case, we refer to a previous computational study in which the thermal conductivity of the DPPC membranes was obtained at different temperature gradients. In the same study, the lowest value of thermal conductivity was reported for a membrane whose leaflets were in two different temperatures, one below the phase transition temperature and the other above it [24]. One of the membrane leaflets in the gel phase and the other in the liquid crystalline phase reveal a form of asymmetry between the two membrane leaflets. Our asymmetric membrane has a rectification factor of 0.008, which is much lower than the previously reported values for archaical membranes [18].

Besides normal asymmetry in the cholesterol content of the two membrane leaflets, a very recent study suggests that external thermal gradients can create asymmetric cholesterol distribution between the two membrane leaflets [44]. The results of the same study indicate that the flip-flop rate of cholesterol, which is a rather small and less polar molecule in comparison with other lipid molecules, is in the order of microseconds or milliseconds. Elsewhere, the cholesterol flip-flop rate is reported to be between 80 ns and 250 ns [43]. However, the timescale of our simulations was much lower (around 20 ns) than the reported values. Therefore, there is almost no chance to observe a cholesterol flip-flop in our simulations.

D. Thermal conductivity and rectification of DPPC membrane containing amyloid precursor protein

To investigate the thermal conductivity of the membrane in the presence of APP, we consider two separate cases (Fig. 9).

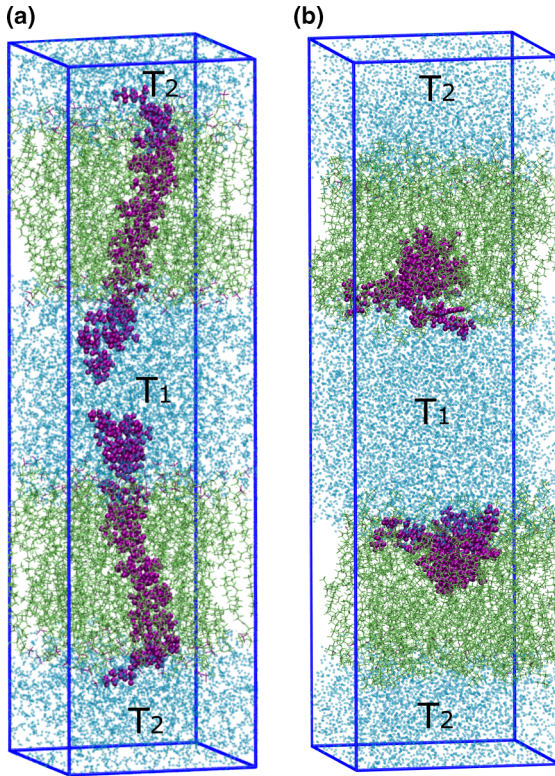


FIG. 9. Two membrane-protein systems. In system a, the transmembrane domain of APP is packed with DPPC molecules. In system b, part of the APP laid down on the lipid membrane. Lipids, protein, and water molecules are colored in green, purple, and cyan, respectively.

In the first model [Fig. 9(a)], the transmembrane domain of APP inserted into the membrane, and in the second one [Fig. 9(b)], part of APP laid on the membrane. For both cases, we study thermal conductivity in the forward and backward directions. Our results suggest that in both cases, the thermal conductivity coefficients in the forward direction are different

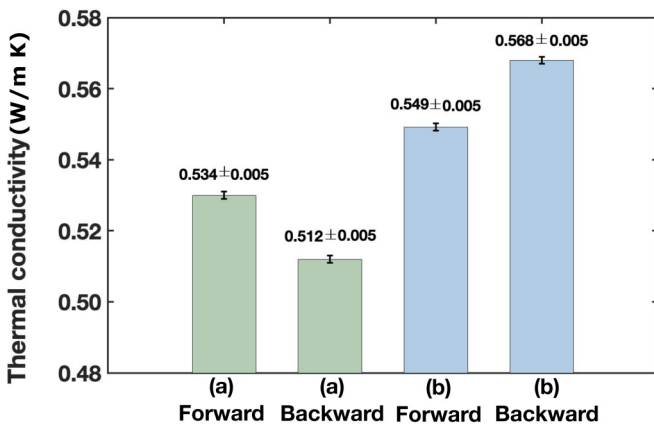


FIG. 10. Thermal conductivity coefficients of the membranes with amyloid precursor protein in the forward and backward directions. The two leftmost columns show the value of thermal conductivity for system a in Fig. 9 and the two rightmost columns show the value of thermal conductivity for system b in Fig. 9.

TABLE III. Thermal conductivity coefficients (κ) and rectification factors (ϵ) are reported at specified temperature differences for the two illustrated models in Fig. 9. In the third and fourth columns, the standard deviations (SD) are specified inside the parentheses.

System	Direction	ΔT (SD) K	κ (SD) $W m^{-1} K^{-1}$	ϵ
a	Forward	76.0 (1.5)	0.534 (0.005)	0.043
	Backward	74.9 (1.2)	0.512 (0.005)	
b	Forward	62.0 (1.1)	0.549 (0.005)	0.033
	Backward	62.5 (0.9)	0.568 (0.005)	

from the ones obtained in the backward direction (Fig. 10). Table III represents the values of thermal conductivity coefficients and the rectification factors for both cases.

We applied a t test to the values of thermal conductivity coefficients in the forward and backward directions for the two membrane-protein systems. According to the results of this test (see Table IV), the values of the thermal conductivity coefficients have a significant difference when measured in the forward direction than the backward direction. The rectification factors we obtain for the two membrane-protein systems are comparable with the previously reported rectification factors for other types of cell membranes (between 0.028 and 0.091) [18].

IV. CONCLUSION

In this study, we applied a reverse nonequilibrium molecular dynamics approach to obtain the thermal conductivity of atomistic models of DPPC membrane with different compositions. We obtained the thermal conductivity of DPPC membrane at four different cholesterol levels. Our study finds a positive correlation between the concentration of cholesterol in the membrane and the membrane thermal conductivity. We relate the increase in the membrane thermal conductivity to the increased structural order in the membrane upon the addition of cholesterol. It is stated elsewhere that the hydrophobic effect of cholesterol is responsible for packing the hydrocarbon chains of lipids (hydrophobic part of lipid molecules) and, therefore, increasing the order in the membrane [45]. The results obtained from our model membrane with an asymmetric distribution of cholesterol in the two membrane leaflets further support this idea. The lower value of thermal conductivity of the asymmetric membrane in comparison with the symmetric membranes indicates the close relationship between the structural order in the membrane and the membrane thermal conductivity.

Furthermore, our simulations suggest that the inclusion of cholesterol to the membrane enhances the hydration of phospholipid head groups. The increased density of

TABLE IV. Result of the t test for thermal conductivity coefficients in the forward (F) and backward (B) directions for the two membrane-protein systems illustrated in Fig. 9.

Name	Mean diff.	Std. err diff.	t	df	Sig. (2-tailed)
System a (F, B)	0.022	0.002	11.299	28.0	$p < 0.05$
System b (F, B)	-0.019	0.001	-13.856	42.0	$p < 0.05$

water molecules at the lipid-water interface enhances the membrane-water interactions which can partly compensate the sharp drop in the local thermal conductivity profile at the lipid-water interface reported in a previous study [14].

It is also evident that cholesterol increases the van der Waals interactions between the hydrocarbon chains of lipids. The increased van der Waals interaction could be responsible for the increased thermal conductivity in the lipid membrane. This is analogous to the increased thermal conductivity of simple fluids at a high density, which is mainly due to the repulsive intermolecular forces [46,47].

For the membranes decorated with APP, we observe a significant difference between the thermal conductivity coefficients in the forward and backward directions. Consequently, there is a rectification effect when heat flows in opposite directions through the membrane-protein system. Many believe that the rectification depends on the temperature difference across the membrane [18]. However, the rectification factors we obtain for the membrane-protein models are more com-

parable with the previously obtained values (between 0.028 and 0.091) for asymmetric archael membranes at $\Delta T = 20$ K [18] than the ones obtained (between 0.1 and 3.5) for carbon nanotubes at $\Delta T = 100$ K [48,49]. We conclude that thermal rectification is more affected by the structure than the temperature gradient, but further studies are required to prove it.

The results of this study shed light on the selective treatment methods, such as photothermal cancer therapy [50]. According to what we report for the specific case of colorectal cells here, normal cells with a large ratio of $[CHL]_o/[CHL]_i$ and a high thermal resistance, can survive during the treatment process.

ACKNOWLEDGMENTS

The authors would like to thank Mahsa Rafiee Alhossaini, Department of Biostatistics, Faculty of Medical Sciences, Tarbiat Modares University, Tehran, Iran, for her contribution to the statistical analysis.

-
- [1] B. Alberts, A. Johnson, J. Lewis, M. Raff, K. Roberts, and P. Walter, *Molecular Biology of the Cell*, 4th ed. (Garland Science, New York, 2002), Vol. 91.
- [2] T. Harayama and H. Riezman, Understanding the diversity of membrane lipid composition, *Nat. Rev. Mol. Cell Biol.* **19**, 281 (2018).
- [3] S.-L. Liu, R. Sheng, J. H. Jung, L. Wang, E. Stec, M. J. O'Connor, S. Song, R. K. Bikkavilli, R. A. Winn, D. Lee *et al.*, Orthogonal lipid sensors identify transbilayer asymmetry of plasma membrane cholesterol, *Nat. Chem. Biol.* **13**, 268 (2017).
- [4] Y. Lange and J. M. Slayton, Interaction of cholesterol and lysophosphatidylcholine in determining red cell shape, *J. Lipid Res.* **23**, 1121 (1982).
- [5] P. L. Yeagle, *The Membranes of Cells* (Academic Press, New York, 2016).
- [6] H. Lodish, A. Berk, S. L. Zipursky, P. Matsudaira, D. Baltimore, and J. Darnell, *Molecular Cell Biology*, 4th ed. (Freeman & Co., New York, 2000).
- [7] A. C. Johansson and E. Lindahl, Protein contents in biological membranes can explain abnormal solvation of charged and polar residues, *Proc. Natl. Acad. Sci. U. S. A.* **106**, 15684 (2009).
- [8] J. A. Lemkul and D. R. Bevan, A comparative molecular dynamics analysis of the amyloid β -peptide in a lipid bilayer, *Arch. Biochem. Biophys.* **470**, 54 (2008).
- [9] A. M. Brown and D. R. Bevan, Molecular dynamics simulations of amyloid β -peptide (1-42): Tetramer formation and membrane interactions, *Biophys. J.* **111**, 937 (2016).
- [10] K. Nadezhdin, O. Bocharova, E. Bocharov, and A. Arseniev, Structural and dynamic study of the transmembrane domain of the amyloid precursor protein, *Acta Naturae* **3**, 69 (2011).
- [11] G. Baffou and R. Quidant, Thermo-plasmonics: Using metallic nanostructures as nano-sources of heat, *Laser Photon. Rev.* **7**, 171 (2013).
- [12] A. R. Bastos, C. D. Brites, P. A. Rojas-Gutierrez, C. DeWolf, R. A. Ferreira, J. A. Capobianco, and L. D. Carlos, Thermal properties of lipid bilayers determined using upconversion nano-thermometry, *Adv. Funct. Mater.* **29**, 1905474 (2019).
- [13] F. Müller-Plathe, A simple nonequilibrium molecular dynamics method for calculating the thermal conductivity, *J. Chem. Phys.* **106**, 6082 (1997).
- [14] T. J. Müller and F. Müller-Plathe, Heat transport through a biological membrane-an asymmetric property? Technical issues of nonequilibrium molecular dynamics methods, *Int. J. Quantum Chem.* **111**, 1403 (2011).
- [15] T. Nakano, G. Kikugawa, and T. Ohara, A molecular dynamics study on heat conduction characteristics in DPPC lipid bilayer, *J. Chem. Phys.* **133**, 154705 (2010).
- [16] T. Nakano, G. Kikugawa, and T. Ohara, Molecular heat transfer in lipid bilayers with symmetric and asymmetric tail chains, *J. Heat Transfer* **135**, 061301 (2013).
- [17] D. Potdar and M. Sammalkorpi, Asymmetric heat transfer from nanoparticles in lipid bilayers, *Chem. Phys.* **463**, 22 (2015).
- [18] S. Youssefian, N. Rahbar, and S. Van Dessel, Thermal conductivity and rectification in asymmetric archael lipid membranes, *J. Chem. Phys.* **148**, 174901 (2018).
- [19] A. M. Smondyrev and M. L. Berkowitz, Structure of dipalmitoylphosphatidylcholine/cholesterol bilayer at low and high cholesterol concentrations: Molecular dynamics simulation, *Biophys. J.* **77**, 2075 (1999).
- [20] F. de Meyer and B. Smit, Effect of cholesterol on the structure of a phospholipid bilayer, *Proc. Natl. Acad. Sci. U. S. A.* **106**, 3654 (2009).
- [21] G. M'Baye, Y. Mély, G. Duportail, and A. S. Klymchenko, Liquid ordered and gel phases of lipid bilayers: Fluorescent probes reveal close fluidity but different hydration, *Biophys. J.* **95**, 1217 (2008).
- [22] T. D. Pollard, W. C. Earnshaw, J. Lippincott-Schwartz, and G. Johnson, *Cell Biology E-Book* (Elsevier Health Sciences, Philadelphia, 2016).
- [23] M. Mahmoudi, A. M. Abdelmonem, S. Behzadi, J. H. Clement, S. Dutz, M. R. Ejtehadi, R. Hartmann, K. Kantner, U. Linne, P. Maffre *et al.*, Temperature: The ignored factor at the nanobio interface, *ACS nano* **7**, 6555 (2013).
- [24] S. Youssefian, N. Rahbar, C. R. Lambert, and S. Van Dessel, Variation of thermal conductivity of DPPC lipid bilayer

- membranes around the phase transition temperature, *J. R. Soc., Interface* **14**, 20170127 (2017).
- [25] S. Jo, T. Kim, V. G. Iyer, and W. Im, CHARMM-GUI: A web-based graphical user interface for CHARMM, *J. Comput. Chem.* **29**, 1859 (2008).
- [26] S. Phimpston, Fast parallel algorithms for short-range molecular dynamics, *J. Comput. Phys.* **117**, 1 (1995).
- [27] A. D. MacKerell Jr, D. Bashford, M. Bellott, R. L. Dunbrack Jr., J. D. Evanseck, M. J. Field, S. Fischer, J. Gao, H. Guo, S. Ha *et al.*, All-atom empirical potential for molecular modeling and dynamics studies of proteins, *J. Phys. Chem. B* **102**, 3586 (1998).
- [28] R. B. Best, X. Zhu, J. Shim, P. E. Lopes, J. Mittal, M. Feig, and A. D. MacKerell Jr., Optimization of the additive CHARMM all-atom protein force field targeting improved sampling of the backbone ϕ , ψ and side-chain χ_1 and χ_2 dihedral angles, *J. Chem. Theory Comput.* **8**, 3257 (2012).
- [29] W. L. Jorgensen, J. Chandrasekhar, J. D. Madura, R. W. Impey, and M. L. Klein, Comparison of simple potential functions for simulating liquid water, *J. Chem. Phys.* **79**, 926 (1983).
- [30] P. J. Barrett, Y. Song, W. D. Van Horn, E. J. Hustedt, J. M. Schafer, A. Hadziselimovic, A. J. Beel, and C. R. Sanders, The amyloid precursor protein has a flexible transmembrane domain and binds cholesterol, *Science* **336**, 1168 (2012).
- [31] H. M. Berman, J. Westbrook, Z. Feng, G. Gilliland, T. N. Bhat, H. Weissig, I. N. Shindyalov, and P. E. Bourne, The protein data bank, *Nucleic Acids Res.* **28**, 235 (2000).
- [32] H. Berman, K. Henrick, and H. Nakamura, Announcing the worldwide protein data bank, *Nature Struct. Mol. Biol.* **10**, 980 (2003).
- [33] M. A. Lomize, I. D. Pogozheva, H. Joo, H. I. Mosberg, and A. L. Lomize, OPM database and PPM web server: Resources for positioning of proteins in membranes, *Nucleic Acids Res.* **40**, D370 (2011).
- [34] A. I. Jewett, Z. Zhuang, and J.-E. Shea, Moltemplate a coarse-grained model assembly tool, *Biophys. J.* **104**, 169a (2013).
- [35] J. R. Silvius, Thermotropic phase transitions of pure lipids in model membranes and their modifications by membrane proteins, *Lipid-Protein Interactions* **2**, 239 (1982).
- [36] G. J. Martyna, M. L. Klein, and M. Tuckerman, Nosé–hoover chains: The canonical ensemble via continuous dynamics, *J. Chem. Phys.* **97**, 2635 (1992).
- [37] H. M. McConnell and A. Radhakrishnan, Condensed complexes of cholesterol and phospholipids, *Biochim. Biophys. Acta (BBA)-Biomembranes* **1610**, 159 (2003).
- [38] J. Ipsen, O. Mouritsen, and M. Bloom, Relationships between lipid membrane area, hydrophobic thickness, and acyl-chain orientational order: The effects of cholesterol, *Biophys. J.* **57**, 405 (1990).
- [39] G. W. Stockton and I. C. Smith, A deuterium nuclear magnetic resonance study of the condensing effect of cholesterol on egg phosphatidylcholine bilayer membranes. I. Perdeuterated fatty acid probes, *Chem. Phys. Lipids* **17**, 251 (1976).
- [40] F. A. Nezil and M. Bloom, Combined influence of cholesterol and synthetic amphiphilic peptides upon bilayer thickness in model membranes, *Biophys. J.* **61**, 1176 (1992).
- [41] A. Kusumi, W. K. Subczynski, M. Pasenkiewicz-Gierula, J. S. Hyde, and H. Merkle, Spin-label studies on phosphatidylcholine-cholesterol membranes: Effects of alkyl chain length and unsaturation in the fluid phase, *Biochim. Biophys. Acta (BBA)-Biomembranes* **854**, 307 (1986).
- [42] H. I. Ingólfsson, M. N. Melo, F. J. Van Eerden, C. Arnarez, C. A. Lopez, T. A. Wassenaar, X. Periole, A. H. De Vries, D. P. Tieleman, and S. J. Marrink, Lipid organization of the plasma membrane, *J. Am. Chem. Soc.* **136**, 14554 (2014).
- [43] S. O. Yesylevskyy and A. P. Demchenko, How cholesterol is distributed between monolayers in asymmetric lipid membranes, *Eur. Biophys. J.* **41**, 1043 (2012).
- [44] J. W. Carter, M. A. Gonzalez, N. J. Brooks, J. M. Seddon, and F. Bresme, Flip-flop asymmetry of cholesterol in model membranes induced by thermal gradients, *Soft Matter* **16**, 5925 (2020).
- [45] S. Bhattacharya and S. Haldar, Interactions between cholesterol and lipids in bilayer membranes: Role of lipid head group and hydrocarbon chain–backbone linkage, *Biochim. Biophys. Acta (BBA)-Biomembranes* **1467**, 39 (2000).
- [46] Y. Ishii, K. Sato, M. Salanne, P. A. Madden, and N. Ohtori, Thermal conductivity of simple liquids: Origin of temperature and packing fraction dependences, *J. Chem. Phys.* **140**, 114502 (2014).
- [47] J. D. Weeks, D. Chandler, and H. C. Andersen, Role of repulsive forces in determining the equilibrium structure of simple liquids, *J. Chem. Phys.* **54**, 5237 (1971).
- [48] J. Hu, X. Ruan, and Y. P. Chen, Thermal conductivity and thermal rectification in graphene nanoribbons: A molecular dynamics study, *Nano Lett.* **9**, 2730 (2009).
- [49] G. Loh, E. H. T. Teo, and B. K. Tay, Thermal rectification reversal in carbon nanotubes, *J. Appl. Phys.* **112**, 103515 (2012).
- [50] G. Eskiizmir, Y. Baskin, and K. Yapıcı, Graphene-based nanomaterials in cancer treatment and diagnosis, in *Fullerenes, Graphenes and Nanotubes*, edited by A. Grumezescu (William Andrew Publishing, USA, 2018), pp. 331–374.

Correction: The penultimate sentence of the second paragraph in Sec. III A contained an error in wording and has been fixed.

Second Correction: The previously published Figures 6, 8, and 10 contained an incorrect unit for thermal conductivity and have been replaced. The unit has also been fixed in the penultimate paragraph of Sec. III A and in Table III.